International Journal of Current Engineering and Technology
ISSN 2277 - 4106

Available at http://inpressco.com/category/ijcet

Research Article

Fracture Toughness Measurement of hot pressed ZrB_2-$MoSi_2$ Composite

Manab Mallik[*Å], Saikat Pan[Å] and Himadri Roy[Ḃ]

[Å]Department of Metallurgical and Materials Engineering, National Institute of Technology, Durgapur - 713209, INDIA
[Ḃ]NDT & Metallurgy Group, Central Mechanical Engineering Research Institute (CSIR), Durgapur, INDIA

Accepted 05 November 2013, Available online 01 December 2013, **Vol.3, No.5 (December 2013)**

Abstract

The fracture toughness of a hot pressed ZrB_2-20 vol.% $MoSi_2$ based ultra high temperature ceramic composite was measured by the Vickers indentation method and single edge notch bend test (SENB). The material was tested for indentation fracture toughness (IFT) at room temperature at four different loads between 49.03 and 196.3 N and four different indentation times between 15 and 30 s. Different formulae that exist to evaluate IFT were compared. The influences of the indentation load and the dwell time on IFT measurement were investigated. Results confirmed that the transformation occur from Palmqvist crack system to median crack system between low load to higher loads. The Palmqvist crack model yielded an IFT of ~3 MPa√m, whereas, the median crack model yielded an IFT of ~3–4 MPa√m. It is seen that the use of actual crack system at a particular test load gives almost similar fracture toughness values which are measured by the standard conventional method.

Keywords: *Borides, Ceramic, Fracture toughness, Hardness.*

1. Introduction

The measurement of the fracture toughness accurately of brittle materials can often be challenging. It can be difficult to create a sharp precrack without catastrophically failing the specimen (Munz, D. *et al* 1980; Ritchie, R. O. *et al* 1990; Fett, T. *et al* 2006). For those reasons, assessing fracture toughness by making direct measurements of cracks created using a sharp diamond indenter, such as Vickers, Knoop, Berkovich, or cube corner, can appear to be an attractive alternative to more traditional fracture toughness testing techniques (Lawn, B. R. *et al* 1980; Anstis, G. R. *et al* 1981; Fett, T. *et al* 2005). Such tests can be relatively quick and easy to perform. The requirement of small sized specimen and ease of specimen preparation have made it popular for evaluating fracture toughness of ceramics and glasses. The indentation fracture toughness measurement involves measurement of the length of the cracks emanating from the corners of Vickers indentation diagonals, the applied indentation load and some material properties like elastic modulus and Poisson's ratio. There is no need for the preparation of the specimens with special geometry and complex notches. The principle of this technique is based on the consideration of two models (Evans, A. G. *et al* 1976) of crack formation mainly as Plamqvist and Median crack systems. The Plamqvist crack system consists of four semi-elliptically shaped cracks whereas the median consists of two halfpenny shaped cracks perpendicular to the plane of indentation. Nihara et al. proposed that Plamqvist and median cracks occur at low and high ratios of crack lengths *l* or *c* to half diagonal lengths of Vickers indentation *a*. In addition, a third category of formulae (Blendell, J. E. 1979; Evans, A. G. 1979; Lankford, J. 1982) referred to as curve fitting approaches is also found in use, evaluation of IFT of brittle solids. These formulae are not influenced by the nature of the cracks associated with an indentation.

The Zirconium diborides (ZrB_2)–based composites are being considered for use as potential candidates for a variety of high–temperature structural applications, including furnace elements, plasma-arc electrodes, or rocket engines and thermal protection structures for leading-edge parts on hypersonic re-entry space vehicles at over 1800 °C (Upadhya, K. *et al* 1997; Brown, A. S. 1997; Norasetthekul, S. *et al* 1999). The potential applicability for these application exhibited by ZrB_2–based composites is due to their unique combination of high melting temperature (>3000 ◦C), high thermal and electrical conductivities (Mallik, M. *et al.* 2012), chemical inertness against molten metals, and good thermal shock resistance (Mitra, R. *et al.* 2009; Mroz, C. 1994; Telle, R. *et al* 2000). The densification of ZrB_2 powders needs very high temperatures (2100–2300 °C) and pressures for sintering procedures due to covalent bond and low self-diffusivity (Pastor, M. 1977). High processing temperature causes coarse microstructures with an amount of residual porosity. It is possible to achieve relative densities and

*Corresponding author: **Manab Mallik**

mechanical properties equivalent to those in the hot-pressed ZrB_2 based composites by carrying out pressureless sintering of ZrB_2 with different SiC content using B_4C and phenolic resin as additives (Mallik, M. *et al.* 2013; Zhang, S. *et al.* 2008).

The addition of nitrides like Si_3N_4 or AlN was found to improve the sinterability, the microstructure and the properties of ZrB_2 by producing an intergranular liquid phase (Monteverde, F. *et al* 2002; Monteverde, F. *et al* 2003; Monteverde, F. *et al* 2005). To improve the mechanical properties and oxidation resistance of zirconium diboride the most promising approach is the addition of 20 vol% of silicon carbide (Levine, S. R. *et al* 2002, Mallik, M. *et al.* 2011). In this study, $MoSi_2$ is selected as a ceramic additive for ZrB_2. The main reason for this choice is that, in oxidizing conditions, $MoSi_2$ provides a silica coating which acts as a protective barrier against high-temperature oxidation of ZrB_2. ZrB_2–$MoSi_2$ ceramics were previously studied and it was found that the addition of 10–30 vol% $MoSi_2$ improved both room temperature mechanical properties (Chamberlain, A. *et al* 2003) and oxidation resistance (Chamberlain, A. *et al* 2003; Sciti, D. *et al* 2005) compared to monolithic ZrB_2 materials. The focus of this work is to determine the indentation fracture toughness (IFT) of ZrB_2–$MoSi_2$ composite and studying the suitability of the existing formulae for evaluating IFT of this composite.

2. Experimental

2.1 Sample Preparation

The material used in this investigation is ZrB_2-$MoSi_2$ (ZM) composite having 20 volume percent $MoSi_2$ particles, was obtained as a courtesy of the Indian Institute of Technology Kharagpur, India. The powders of ZrB_2 and $MoSi_2$ were obtained from H.C. Starck, Germany. The powder samples of ZrB_2-20 vol% $MoSi_2$ (ZM) were mixed in the Planetary Mono Mill (model Pulverisette 6, Fritsch, Germany) at a milling speed of 250 rpm for 2 h. The powders were wrapped in grafoil, placed in a cylindrical graphite die, and subsequently hot pressed inside a resistance furnace (DR. Fritsh GMBH D-70736 Fallback) in vacuum at 1800 ^oC for 30 min using a uniaxial pressure of 30 MPa.

2.2 Sample Characterization

The hot pressed billets were sectioned using an Isomet slow speed diamond saw cutter (Buehler Ltd, USA). The sectioned samples were initially polished, first on coarse and fine diamond coated discs, subsequently on abrasive SiC papers down to 600 grit, and finally on clothes smeared with 6, 1 and 0.25 μm diamond lapping paste. The densities of the hot pressed billets were measured using the Archimedes principle with water as the immersing medium. The different phases present in the composite were identified by X-ray diffraction (XRD) technique using Cu Kα radiation. The microstructures of the polished samples were studied using scanning electron microscope (FESEM, Model: SUPRA 40, ZEISS) equipped with Energy Dispersive X-Ray (EDX) microanalyser (Model: ISIS300, Oxford Instrument Ltd., UK).

The elastic moduli and Poisson's ratio were calculated using the longitudinal and transverse wave's velocities in the samples obtained by ultrasonic technique (Panametrics-NDT, Epoch). The Vickers hardness was measured using a diamond indenter operated with five different loads between 2.94 N and 294.2 N for 15 seconds. The indentation fracture toughness (IFT) values were measured using a diamond indenter at four different loads between 47.03 N and 196.13 N for 15 s. A series of indentations were produced using different applied loads. The lengths of cracks at corners of indentations were measured using scanning electron microscope to determine the indentation fracture toughness. The values of average indentation diagonals were obtained from at least 10 readings at each load level. The average crack lengths were measured along both the diagonal directions at least 40 readings at each load level. In addition to that, a series of IFT experiments were also done at 98.07 N loads for different indentation time t_{id} duration of 15, 20, 25 and 30 s.

In addition to the IFT, the fracture toughness of the investigated composite was also measured using a SENB specimen having dimensions of 4 mm (thickness) × 8 mm (width) × 36 mm (length), and ~ 4 mm deep notch. The test was carried out with a crosshead speed of 0.1 mm per min on a three point bend fixture with a span of 32 mm. The fracture toughness, K_{IC} was determined using the equation (1):

$$K_{IC} = [PS/BW^{1.5}].f\,(a/W). \quad (1)$$

where P is the load, S is the span, B is the thickness, W is the width, a is the initial crack length, and $f(a/W)= [3(a/W)^{0.5}/2\{1-(a/W)\}^{1.5}\{1+(2a/W)\}]\times[1.99-(a/W)(1-a/W)\{2.15-3.93(a/W)+2.7(a/W)^2\}]$.

3. Results and Discussion

3.1 Microstructure

The density, hardness and elastic properties, of the investigated composite have been presented in Table 1. The density of the ZM composite has been found to be 5.8 $g.cm^{-3}$, which is 94% of the theoretical density calculated from the rule of mixtures. XRD pattern of the ZM composite confirm the constituent phases present in composite (Fig. 1). The microstructure of the ZM is shown in Fig. 2. The SEM image clearly shows uniform distribution of phases in the microstructure. The ZrB_2 phase appears bright, while the $MoSi_2$ looks gray. The identity of the major elements in each of these constituents was confirmed by EDX analysis.

3.2 Hardness

For IFT calculations, it is recommended to take into account the true (load independent) hardness of the

Table 1: Density, hardness and elastic properties of ZM composite.

Density (g/cm^3)	5.8
Hardness (GPa)	16.01
Young's modulus (GPa)	455.3
Young's modulus (ROM) (GPa)	485
Poisson's ratio	0.11

material (Ray, K. K. et al 1999; Gong, J. *et al* 2002). It is well known that the apparent hardness decreases with the increase of the indentation load and approaches a constant value at a relatively high load level (Fig. 3). At low loads the hardness is usually highly dependent on the load, as illustrated in Fig. 3. The measurement of the Vickers hardness above 50 N may be influenced by the indentation crack formation. Li *et al*. reported that the measurement of the Vickers microhardness for α -SiC above 3 N was influenced by the indentation crack formation. However, once the indentation cracks are fully developed for the Vickers indentations, then Vickers microhardness appears to be constant and consistent (Li, Z. *et al* 1989). For the ZrB_2-$MoSi_2$ the Vickers hardness below 50 N is highly load dependent and above 50 N (indentation cracks are fully developed), Vickers hardness shows almost constant value which has been taken for IFT measurement. The magnitude of hardness for the ZrB_2-20 vol. % $MoSi_2$ composite has been found to be 16.01 GPa. Comparison of the measured hardness data with the hardness values for hot pressed ZrB_2-20 vol. % $MoSi_2$ composite reported by Guo *et al.* (16.3 GPa) shows that experimentally obtained value is ~2% lower. The earlier investigator (Gou, S. Q. et al 2008) estimated the hardness of ZrB_2-20 vol. % $MoSi_2$ composite having 99.8 % relative density and hence this is expected to be main reason for getting higher hardness value.

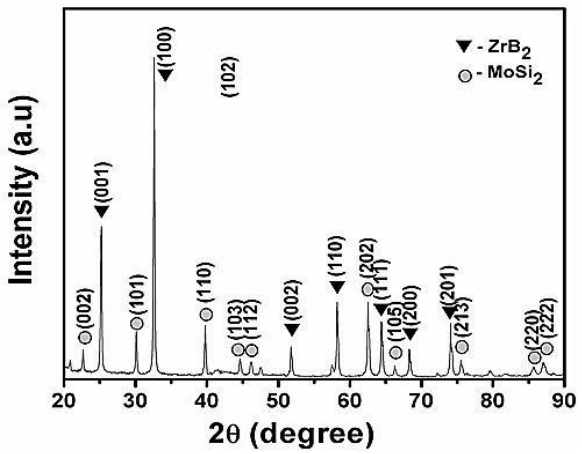

Fig. 1: Plot showing the XRD pattern of the ZM composite.

3.3 Fracture Toughness

The estimates of fracture toughness have been made using measured crack lengths and Vickers' indentation diagonals, estimated hardness values of the specimen, calculated elastic modulus, Poisson's ratio and suggested values of constants incorporated in the various formulae. Figure 3 (inset) illustrates typical crack patterns which were obtained from the Vickers indentation at 196.13 N loads. Figure 3(inset) depicts a nearly perfect crack pattern with a symmetrical indentation having four cracks of almost similar crack lengths. The characteristic lengths, *a* and *c*, obtained from the perfect crack patterns using Vickers indentations and the long diagonals, *d* values are measured. The various formulae using IFT calculation are listed in Table 2 and are numbered 1-9 for convenience in the subsequent discussion.

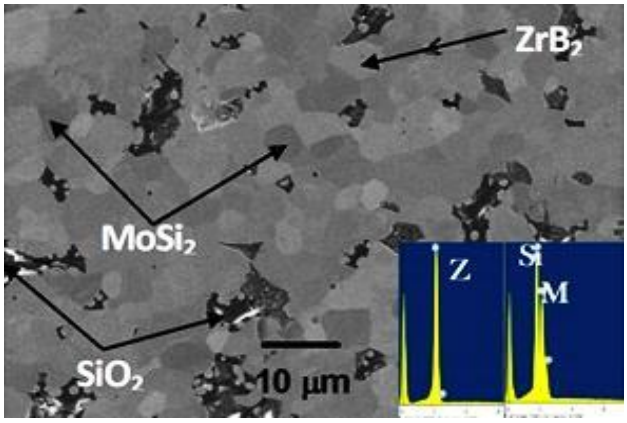

Fig. 2: SEM (BSE) image of ZM composite showing ZrB_2 of light-grey phase, $MoSi_2$ of intermediate-grey phase, and SiO_2 phase with the darkest contrast.

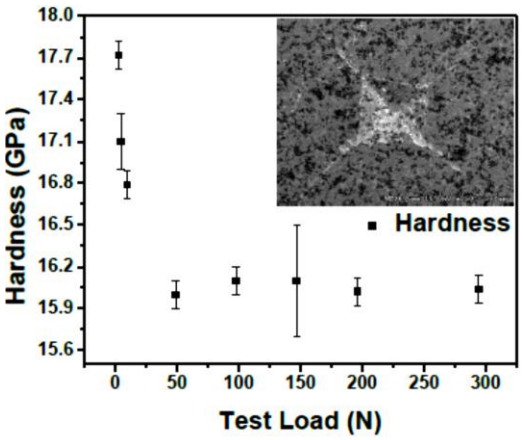

Fig. 3: Plot represents the Vickers hardness as a function of load and typical indentation crack patterns at test loads 196.13 N.

The influence of test loads on IFT is summarized in Figs. 4(a & b). Figure 4(a) illustrates that almost load independent K_{IC} values are calculated using Palmqvist crack system formulae (2–4) whereas; Fig. 4(b) represents the K_{IC} values which are determined using Median crack system (5–10). The values decrease as the test loads increases from 47.03 N to 98.07 N, and with further increase in load almost load independent K_{IC} values are obtained. These results reveal that the variation of the K_{IC} values calculated from the different proposed formulae is quite large, from 3 to 9 MPa√m. As many of the formulae

have the same terms, the only real difference is their coefficient. These indentation fracture toughness values do not match with value (3.74 MPa√m) obtained from SENB test. The value of SENB test is similar to that reported by Balbo and Sciti using the chevron-notched beam (CNB) specimen technique or 4 MPa√m reported by Silvestroni and Sciti using the CNB specimen technique. Therefore, the results of indentation fracture toughness measurements yield apparent fracture toughness for ZrB_2- 20 vol. % $MoSi_2$ composite are high relative to other more reliable conventional measurement techniques. Fracture toughness measurement involves Palmqvist crack system toughness formulae do not yield the correct magnitude for the fracture toughness of ZrB_2- 20 vol. % $MoSi_2$ in this study. The absolute values of the fracture toughness which are calculated from the median crack model formulae may seem approximately correct. Therefore the correct system or crack pattern is required to be found out. The fractograph of the ZM composite, depicted in Fig. 5, suggests a mixed intergranular and transgranular mode of failure. Some grain facets and river patterns is also observed.

Table 2 Formulae for evaluation of IFT

Nos.	Formulae	References
	Palmqvist crack system	
2.	$K_{IC}=0.0515(P/c^{3/2})$	11
3.	$K_{IC}=0.048(l/a)^{-1/2}(H/E\Phi)^{-2/5}(Ha^{1/2}/\Phi)$	12
4.	$K_{IC}=\beta(HP/4l)^{1/2}, \beta=1/[3(1-\nu^2)(2^{1/2}\Pi tan\psi)^{1/3}]$	13
	Median crack system	
5	$K_{IC}=0.0726(P/c^{3/2})$	11
6	$K_{IC}=0.0752(P/c^{3/2})$	14
7	$K_{IC}=0.129(c/a)^{-3/2}(H/E\Phi)^{-2/5}(Ha^{1/2}/\Phi)$	15
8	$K_{IC}=0.014(E/H)^{1/2}(P/c^{3/2})$	4
9	$K_{IC}=0.014(E/H)^{1/2}(P/c^{3/2})$	5
10	$K_{IC}=0.0725(P/c^{3/2})$	16

E= Elastic modulus; H= Hardness; Φ= Constant (~3); ν= Poisson's ratio; ψ= Half angle of the Vickers indenter, equal to 68º.

Crack patterns which can be induced in solids by Vickers indenter have been distinguished as two distinct types of crack systems. One is the median crack system, which consists of two half penny shaped cracks, and the other is the Palmqvist crack system, which consists of four semielliptical shaped cracks. During Vickesrs indentation test, the median crack develops on ceramics with low fracture toughness values. However, the Palmqvist crack system has also been observed at low loads (Li, Z. *et al* 1989).The two crack systems can be distinguished by their load and crack length, *c* or *l* relationships. For median cracks (Breval, E. *et al* 1985): $c=AP^{2/3}$ whereas, for the Plamqvist cracks (Shetty, D. K. *et al* 1985): $l=BP$ where *c* and *l* are crack lengths. The *A* and *B* are constants which include the *E*, *H* and K_{IC} of the material and the geometric shape of the indenter.

The relationships between *c* or *l* and *P* reveals that the *P–c* profiles of the Palmqvist and median crack systems are indeed very similar. It can be very difficult to differentiate between the two types of crack systems. The experimental results in this study are almost perfectly fitted by the median crack system with better R^2 value 0.99314 than Palmqvist crack system with R^2 value 0.98503.

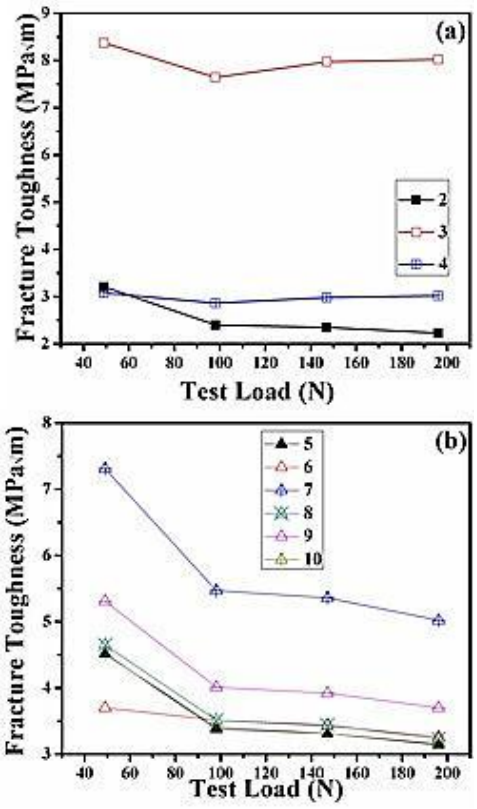

Fig. 4: The load dependence of the IFT calculated using formulae 2-10 (a) Palmqvist crack system, and (b) Median crack system

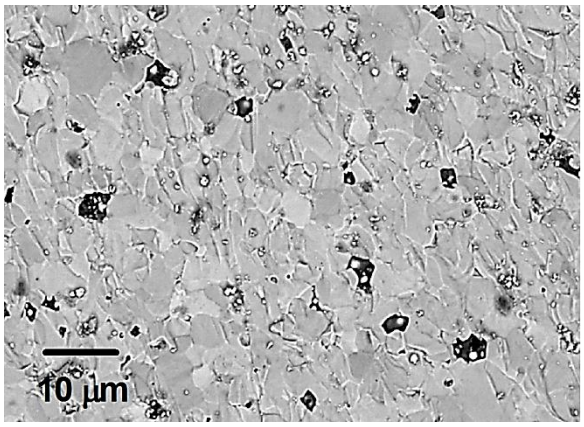

Fig. 5: The fractograph of ZM composite

Further, Niihara et al. proposed that median cracks are considered to be predominant when $c/a \geq 2.5$ i. e. at high loads. In this study, *c/a* values at 49.03 N, 98.07 N, 147.10 N and 196.13 N are 2.26, 3.09, 3.35 and 3.67, respectively. These results confirm that the transformation occur from

Palmqvist crack system to median crack system between low load (49.03 N) to higher loads (≥ 98.07 N). The five formulae include 2, 4, 5, 6, 8, and 9 in Table 3 yield fracture toughness values between 3 to 4 MPa√m. Fig. 6 represents the load vs. K_{IC} plots which are calculated using Palmqvist crack system formulae at lower load and median crack system formulae at higher loads. It is seen that the use of actual crack system at a particular test load gives almost similar fracture toughness values which are very close to fracture toughness values estimated using the SENB specimen technique as well as fracture toughness values reported by earlier researchers (Balbo, A. et al 2008; Silvestroni, L. et al 2007).

Table 3: Summary of K_{IC} Values Calculated using Actual Crack Pattern at Different Loads

Formula. No.	K_{IC}			
	Plamqvist crack system	Median crack system		
	Indentation loads (N)			
	49.03	98.07	147.10	196.13
2	3.21±0.04	—	—	—
4	3.08±0.05	—	—	—
5	—	3.38±0.04	3.31±0.05	3.15±0.03
6	—	3.51±0.04	3.43±0.05	3.26±0.02
8	—	3.51±0.04	3.44±0.04	3.23±0.04
9	—	4.01±0.02	3.92±0.03	3.7±0.02

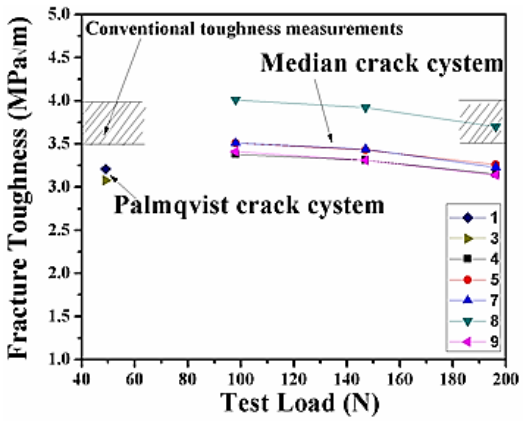

Fig. 6: Fracture toughness calculated using actual crack pattern at different loads

Conclusions

The influences of the indentation load and the dwell time on the fracture toughness measurement have been investigated. The major conclusions are

1. The hot pressed sample had a density 94% of the theoretical density (TD) and microstructure contained ZrB_2 and $MoSi_2$.
2. The hardness value and elastic modulus for ZrB_2 20 vol.% $MoSi_2$ are 16 GPa and 455 MPa, respectively.
3. Using the load versus crack length curves, the Palmqvist crack pattern has been found to occur at test load of 49.03 N.
4. The transformation occurs from Palmqvist crack system to median crack system between low loads (49.03 N) to higher loads (≥ 98.07 N).
5. The Palmqvist crack model yielded an IFT of ~3 MPa√m at 49.03 N indentation load, whereas, the median crack model yielded an IFT of ~3-4 MPa√m at higher loads (≥ 98.07 N) of indentation.

Acknowledgements

The author wishes to acknowledge to Prof. R. Mitra and Prof. K. K. Ray, Department of Metallurgical and Materials Engineering, IIT Kharagpur for providing the materials in the present investigation and their valuable suggestions.

References

Anstis, G. R., Chantikul, P., Lawn, B. R. and Marshall, D. B. A (1981), critical evaluation of indentation techniques for measuring fracture toughness – I. Direct crack measurements. *J. Am. Ceram. Soc.*, 64, 533–538.

Balbo, A. and Sciti, D., Spark plasma sintering and hot pressing of ZrB_2–$MoSi_2$ ultra-high-temperature ceramics, *Mat. Sc. Engg.*, A 2008, 475, 108–112.

Blendell, J. E. The origins of internal stresses in polycrystalline alumina and their effects on mechanical properties. *PhD Thesis. MTI Press, Cambridge, MA*, 1979.

Breval, E., Dodds, G. C. and Macmillan, N. H., (1985), The Hardness, Stiffness nad Toughness of Diplastic Abrasive Materials Prepared by Sol–Gel Techniques, *Mater. Res. Bull.*, 20, 4, 413–129.

Brown, A. S., (1997), Hypersonic designs with a sharp edge. *Aerospace Am.*, 35(9), 20–21.

Chamberlain, A. Fahrenholtz, W. G. G. E. and Ellerby, D. T. Characterization of Zirconium Diboride-Molybdenum Disilicide Ceramics, in Advances in Ceramic Matrix Composites IX, Ceramic Transactions, Volume 153, ed. by N.P. Bansal, J.P. Singh, W.M. Kriven, and H. Schneider, The American Ceramic Society, Westerville, OH 2003, 299–308.

Evans, A. G. and Charles, E. A. (1976), Fracture toughness determinations by indentation. *J. Am. Ceram. Soc.*, 59, [7–8], 371–372.

Evans, A. G. (1979), Fracture toughness: the role of indentation techniques. In *Fracture Mechanics Applied to Brittle Materials* (Freiman, W., ed.). ASTM STP 678, West Conshohocken, PA, 112–135.

Fett, T., Njiwa, A.B.K. and Rodel, J. (2005), Crack opening displacements of Vickers indentation cracks. Engineering Fracture Mechanics, 72, 647–659.

Fett, T., and Munz, D. (2006), Influence of narrow starter notches on the initial crack growth resistance curve of ceramics. *Arc. App. Mech.*, 76, 667–679.

Gong, J., Wang, J. and Guan, Z. (2002), Indentation toughness of ceramics: a modified approach. *J. Mater. Sci.*, 37, 865–869.

Guo, S. Q., Nishimura, T., Mizuguchi, T., and Kagawa, Y. (2008), Mechanical properties of hot-pressed ZrB_2–$MoSi_2$–SiC composites, *J. Euro. Ceram. Soc.*, 28, 1891–1898.

Lankford, J. (1982), Indentation microfracture in the Palmqvist crack regime: implications for fracture toughness evaluation by the indentation method. *J. Mater. Sci. Lett.*, 1, 493–495.

Lawn, H. R. and Fuller, E. R. (1975), Equilibrium penny-like cracks in indentation fracture. *J. Mater. Sci.*, 1975, 10, 2016–2024.

Lawn, B. R., Evans, A. G. and Marshall, D. B. (1980), Elastic/plastic indentation damage in ceramics: the median/radial crack system. *J. Am. Ceram. Soc.*, 1980, 63, 574–581.

Levine, S.R., Opila, E.J., Halbig, M.C., Kiser, J.D., Singh, M. and Salem, J.A. (2002), Evaluation of ultra-high temperature ceramics for aeropropulsion use, *J. Eur. Ceram. Soc.*, 22, 2757–2767.

Li, Z., Ghosh, A., Kobayashi, A. S. and Bradt, R. C. (1989), Indentation fracture toughness of sintered silicon carbide in the Palmqvist crack regime. *J. Am. Ceram. Soc.*, 72, 904–911.

Mallik, M. Ray, K.K. and Mitra, R., (2011), Oxidation behavior of hot pressed ZrB_2–SiC and HfB_2–SiC composites, *J. Eur. Ceram. Soc.*, 31, 199-215.

Mallik, M. Ray, K. K. and Mitra, R. (2012), Electrical and thermophysical properties of ZrB2 and HfB2 based composites, *J. Eur. Ceram. Soc.*, 32, 2545-2555.

Mallik, M. Roy, S. Ray, K. K. and Mitra, R., (2013), Effect of SiC content, additives and process parameters on densification and structure-property relations of pressureless sintered ZrB_2-SiC composites, *Ceram. Int.*, 39, 2915-2932.

Mitra, R. Upender, S. Mallik, M. Chakraborty, S. and Ray, K. K. (2009), Mechanical, thermal and oxidation behavior of zirconium diboride based ultra-high temperature ceramic composites, Key Engg. Mat. 395 55–68.

Monteverde, F. and Bellosi, A. (2002), Effect of the addition of silicon nitride on sintering behavior and microstructure of zirconium diboride. *Scripta Mater.*, 46, 223–228.

Monteverde, F. and Bellosi, A. (2003), Beneficial effects of AlN as sintering aid on microstructure and mechanical properties of hot-pressed ZrB_2. *Adv. Eng. Mater.*, 5(7), 508–512.

Monteverde, F. and Bellosi, A. (2005), Development and characterization of metal diboride- based composites toughened with ultra-fine sic particulates. *Solid State Sci.*, 7, 622–630.

Mroz, C. (1994), Zirconium diboride. *Am. Ceram. Soc. Bull.*, 73(6), 141–142.

Munz, D., Bubsey, R.T. and Shannon Jr., J.L. (1980), Fracture toughness determination of Al_2O_3 using four-point-bend specimens with straight-through and chevron notches, *J. Am. Ceram. Soc.*, 63, 300–305.

Niihara, K., Morena, R. and Hasselman, D. P. H. (1982), Evaluation of K_{IC} of brittle solids by the indentation method with low crack-to-indent ratios. *J. Mater. Sci. Lett.*, 1, 13–16.

Niihara, K. (1983), A fracture mechanics analysis of indentation-induced Palmqvist crack in ceramics. *J. Mater. Sci. Lett.*, 2, 221–223.

Norasetthekul, S., Eubank, P. T., Bradley,W. L., Bozkurt, B. and Stucker, B., (1999), Use of zirconium diboride–copper as an electrode in plasma applications. *J. Mater. Sci.*, 34(6), 1261–1270.

Pastor, M. (1977), Metallic borides: preparation of solid bodies. sintering methods and properties of solid bodies. In *Boron and Refractory Borides*, ed. V. I. Matkovich. Springer, New York, pp. 457–493.

Ray, K. K. and Dutta, A. K. (1999), Comparative study on indentation fracture toughness evaluations of soda-lime-silica glass. *Brit. Ceram. Trans.*, 98, 165–171.

Ritchie, R.O., Dauskardt, R.H., Yu, W. and Brendzel, A.M. (1990), Cyclic fatigue-crack propagation, stress-corrosion, and fracture- toughness behavior in pyrolytic carbon-coated graphite for prosthetic heart valve applications. *J. Bio. Mat. Res.*, 24, 189–206.

Sciti, D., Brach, M. and Bellosi, A. (2005), Oxidation behaviour of a pressureless sintered ZrB_2–$MoSi_2$ ceramic composite, *J. Mater. Res.* 20, 4, 922–930.

Shetty, D. K., Wright, I. G., Mincer, P. N. and Clauer, A. H. (1985), Indentation fracture of WC-Co cermets. *J. Mater. Sci.*, , 20, 1873–1882.

Silvestroni, L. and Sciti, D. (2007), Effects of $MoSi_2$ additions on the properties of Hf– and Zr–B_2 composites produced by pressureless sintering, *Scripta Mater.*, 57, 165–168.

Tanaka, K. (1987), Elastic/plastic indentation hardness and indentation fracture toughness: The inclusion core model. *J. Mater. Sci.*, 22, 1501–1508.

Telle, R., Sigl, L. S. and Takagi, K., (2000), Boride-based hard materials. In *Handbook of Ceramic Hard Materials*, ed. R. Riedel. Wiley–VCH, Wiinheim, Germany, pp. 803–945.

Upadhya, K., Yang, J.-M. and Hoffmann, W. P., (1997), Materials for ultrahigh temperature structural applications. *Am. Ceram. Soc. Bull.*, 76(12), 51–56.

Zhang, S. Hilmas, G.E. and Fahrenholtz, W.G., (2008), Pressureless sintering of ZrB_2–SiC ceramics, *J. Am. Ceram. Soc.*, 91 26–32.